

PAPER • OPEN ACCESS

Effect of joint-edge quality on mechanical properties of laser welded IN718

To cite this article: S Parchegani *et al* 2025 *IOP Conf. Ser.: Mater. Sci. Eng.* **1332** 012012

View the [article online](#) for updates and enhancements.

You may also like

- [Effects of overlap rate and energy density on mechanical properties of Inconel 718 by multiple small-spot-LSP impacts](#)
Woyun Lv, Zhanqiang Liu, Yang Hua *et al.*
- [Laser additive manufacturing of bimetallic structure from TC4 to IN718 via Ta/Cu multi-interlayer](#)
Chenyang Wang, Chun Shang, Zhanqi Liu *et al.*
- [Effect of two-stage solution on microstructure and mechanical property of IN718 alloy fabricated by selective laser melting](#)
Wei Tian, Yu Cao and Li Wang



The Electrochemical Society
Advancing solid state & electrochemical science & technology



249th
ECS Meeting
May 24-28, 2026
Seattle, WA, US
Washington State
Convention Center

Spotlight Your Science

**Submission deadline:
December 5, 2025**

SUBMIT YOUR ABSTRACT

Effect of joint-edge quality on mechanical properties of laser welded IN718

S Parchegani^{1,*}, H Piili¹, A Salminen¹

¹ Department of Mechanical and Materials Engineering, Digital and Surface Engineering Group (DMS), University of Turku (UTU), Turku, Finland.

* Email: saeid.parcheganichozaki@utu.fi

Abstract. Studies on laser welding of metals have shown that the joint-edge quality such as surface roughness and geometry could influence the weld penetration and efficiency thus impacting its mechanical properties. In this study, laser welding was used to join IN718 sheet plates (3.2 mm in thickness) in a butt-joint configuration. The joint edges were prepared with two different methods of laser cutting and standard milling to investigate the effect of joint-edge quality on the mechanical properties of the weld. The laser-cut joints showed a larger fusion zone (FZ) area due to their higher surface roughness. The mechanical properties such as hardness, ultimate tensile strength (UTS), and yield strength were comparable regardless of the joint-edge differences. However, the laser-cut joint showed inferior fatigue strength, assessed at 10^6 cycles, due to micro cracks (microfissures) in the heat affected zone (HAZ).

1. Introduction

The price of laser sources, particularly fiber lasers, has been declining rapidly over the past decade due to the increased market competition and advancement in technological tools used for manufacturing such laser sources [1]. This has made laser sources one of the most attractive technologies for cutting application as the high-power fiber lasers are getting more affordable and accessible. Laser cutting compared to other methods such as plasma and traditional milling could provide higher cutting speed with a high-quality cut edge depending on the parameters [2]. However, other studies have reported that the laser cut edge could impact the fatigue strength of the welded component due to its thermal impact on the HAZ [3]. This is because HAZ of a laser cut edge generally poses higher hardness than the base metal that could result in embrittlement of the weld and reduce the fatigue strength [3]. Therefore, this study aims to provide insights into the impact of two different edge qualities, laser cut edge and standard milling on the mechanical properties of the IN718 welds. In this regard, the tensile and fatigue strength of the welded IN718 were evaluated, and the fracture surface of the welds were analyzed.

2. Materials and methods

2.1 Materials

The IN718 sheet metal were purchased from HARLD PIHL AB (Sweden) in cold-rolled and solution annealed condition (ASTM B670-07). The samples were cut to the size of 100×50×3.2 mm using a 3kW laser with N₂ cutting gas and some of them were kept in the laser cut edge condition and some were further machined to reach a standard milled edge condition. The chemical composition of the wrought IN718 was provided by the manufacturer and is displayed in Table 1.

Table 1. Chemical composition of the wrought Alloy 718 (wt.%).

Element	Ni	Fe	Cr	Mo	Ti	Nb	Mo	Al	B	C
IN718	53.49	18.03	18.23	3.00	1.04	5.17	3.00	0.46	0.002	0.03



2.2 Laser welding

Laser welding of the samples was conducted using a 10 kW IPG fiber laser with a wavelength of 1070 nm. The laser beam was delivered to the work piece using a 300 μm fiber and 400 mm focal lens. The setup provided a top hat beam shape with 800 μm focal point diameter. A coaxial shielding gas nozzle was used on the top surface of the samples to prevent oxidation during welding. Argon gas with a flow rate of about 20 L/min was used as a shielding gas and the coaxial nozzle was set at 5 mm above the samples. The laser welding parameters were set at 3.0 kW power, 3.0 m/min welding speed and the focal point position of -2 mm below the top surface of the samples [4]. The welds are labeled as listed in Table 2.

Table 2. Abbreviations used for welds.

Sample ID	Description
M weld	The weld between wrought IN718 samples with milled edge joint
L weld	The weld between wrought IN718 sample with laser cut edge joint
BM	Base metal of wrought IN718

2.3 Material characterization

The cross-section of the welds was ground and polished using 200-800 grit SiC papers. The micrographs of the cross-section were analyzed using a Wild M400 optical microscope. Microstructural analysis was carried out using a Thermo Scientific Apreo S electron scanning microscope. The microhardness measurement was done using a Struers DuraScan 70 in accordance with EN ISO 6507 standards with an applied load of 2 kgf and a holding duration of 10 seconds. The tensile tests were performed at room temperature utilizing a ZwickRoell tensile machine with a specified force capacity of 100 kN and displacement rate of 0.025 mm/s. For each weld, three tensile samples were evaluated, and the average results for ultimate tensile stress (UTS), 0.2% offset yield stress, and elongation were reported. Fatigue test were performed using a servo hydraulic machine with a stress ratio of $R = 0.1$ and a frequency of about 90 Hz. Three specimens per weld were used to evaluate the fatigue strength at $N = 10^6$ cycles using the method described by Maxwell et al [5]. The surface roughness and pattern of the cut edges were measured using an Alicona InfiFocus optical surface measurement according to ISO 12781-1-2003 standard on a 2.5mm \times 6mm area. Accordingly, the average surface roughness S_a , the root-mean square S_q , and the maximum peak height S_p , were reported.

3. Results and discussion

3.1 Cut edge morphology

The surface pattern and roughness of the joint edges are presented in Figure 1. The laser cut edge shows an average surface roughness of ($S_a = 6.5 \mu\text{m}$, $S_q = 8.8 \mu\text{m}$, $S_p = 35 \mu\text{m}$) which is caused by the rough striations of the laser cutting process as shown in Figure 1b, whereas the milled cut shows a very clean and smooth surface with an average surface roughness of ($S_a = 0.35 \mu\text{m}$, $S_q = 0.54 \mu\text{m}$, $S_p = 3.5 \mu\text{m}$) caused by the rotation of the milling tool (Figure 1a).

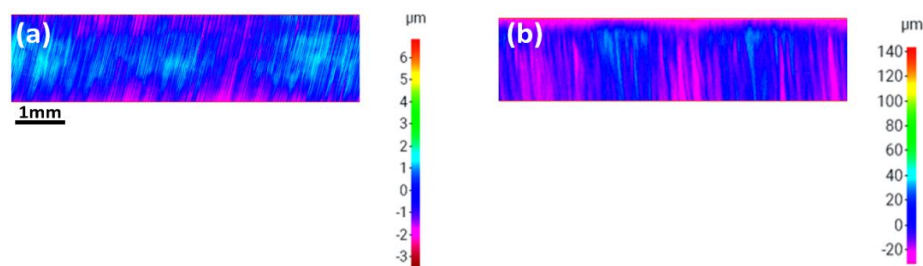


Figure 1. Surface roughness and pattern of milled edge (a) and laser cut edge (b).

3.2 Weld bead geometry

The cross-section macrograph of the welds is depicted in Figure 2. The welds are fully penetrated and free from defects and cracks, demonstrating a good weldability of the IN718 samples using the optimized parameters in this study. Both welds are categorized as weld quality level B according to ISO 13919-1 standard which is the highest weld quality. The L weld shows on average 10% larger FZ area than the M weld as a result of the different surface roughness of the joint edges (section 3.1). It is reported that the higher surface roughness could result in higher absorptivity of the laser beam, thus increasing the FZ area [6]. For example, Farokhi et al [7] reported that the laser welding of 25mm steel samples with laser cut edge require less laser energy than the same samples prepared with milling and water jet cutting due to the surface roughness differences.

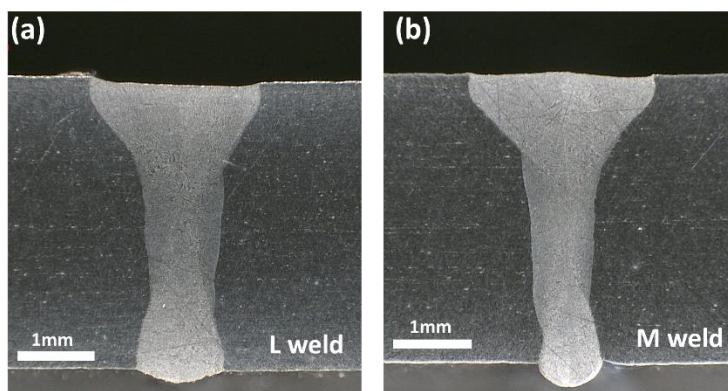


Figure 2. Cross-section macrograph of L weld (a) and M weld (b).

3.3 Microstructure characterization

The microstructure of the base metal IN718 and the FZ is shown in Figure 3. It can be seen that the base metal has a homogenized crystallography with a very fine grains as shown in Figure 3a. The solution annealing resulted in dissolution of the secondary phases in the base metal, however, some very fine and discrete particles are present in the matrix which are reported to be MC phases that are dissolved at much higher temperature than the solution annealing done on the current study samples [8]. The FZ displays a dendrite microstructure with secondary phases that are distributed on the interdendritic regions (Figure 3b). The secondary phases are reported to be Laves and MC in other similar studies [8]. The Laves phases are brittle and hard phases that could act as a suitable site for cracking thus degrading the mechanical properties of the weld [8]. Sumit et al. [9] demonstrated that using low heat input laser energy could result in less Laves phases precipitation in the matrix due to higher solidification rate thus improves the mechanical properties of such a weld.

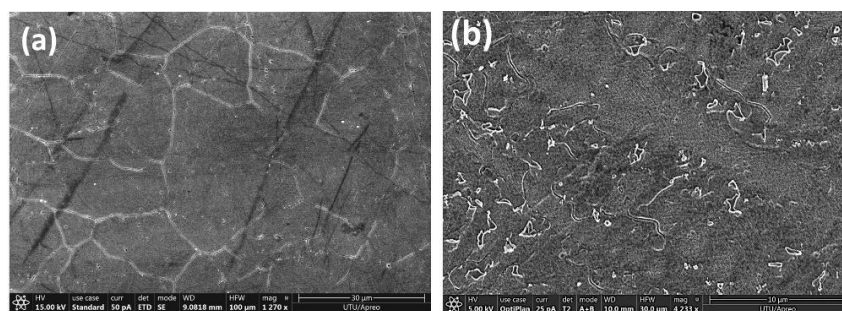


Figure 3. Microstructure of the base metal IN718 (a) and the FZ of M weld (b).

The interface between the FZ and HAZ of the welds are depicted in Figure 4. It can be seen that both welds show some cracks next to the fusion lines. However, the cracks are larger in the L weld (note

the scale difference). These cracks are formed from liquation of secondary phases of MC carbides at the grain boundaries due to the thermal impact of the laser welding in the HAZ [8]. The liquid grain boundary undergoes tensile stress during solidification stage of the welding. As a result, micro cracks (microfissures) form near the fusion line of the welds. The larger cracks at the HAZ of the L weld could be attributed to the thermal impact of the both laser cutting and laser welding process which in turns impacts the microstructure of the HAZ. Further investigation is needed to understand the microstructure changes of the HAZ of the welds.

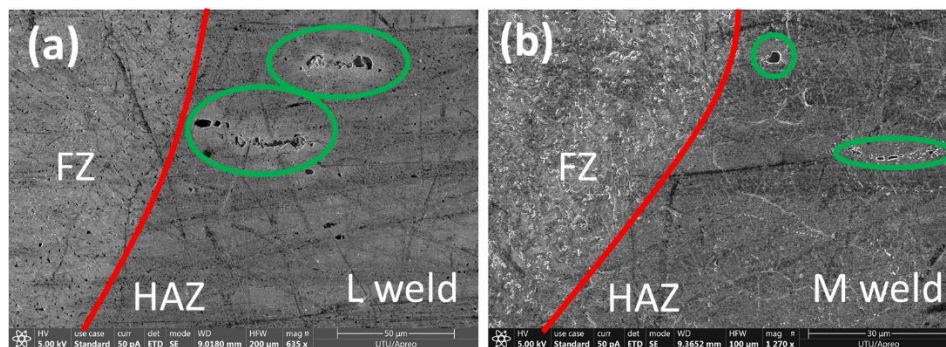


Figure 4. Interface images between the FZ and HAZ in L weld (a) M weld (b).

3.4 Mechanical properties

The microhardness values across the welds and the base metal are presented in Figure 5. The base metal has an average microhardness of 220 ± 3 HV. The FZ of the both welds indicate higher microhardness than that of the base metal with an average microhardness of 270 ± 5 HV and 262 ± 4 HV for the M and L welds respectively. The higher hardness at the FZ is attributed to the presence of Laves phases that are hard particles thus increasing the hardness of the matrix [10]. The M weld shows slightly higher microhardness than the L weld at the FZ that could be attributed to different volume fraction of Laves phases precipitated at the FZ.

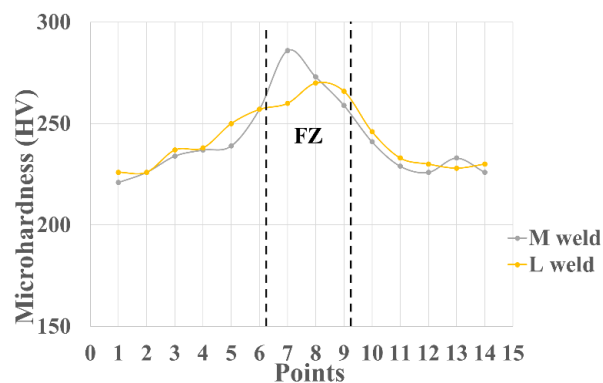


Figure 5. Microhardness values across the welds and BM.

The ultimate tensile strength, yield strength and elongation at break of the welds are displayed in Figure 6. The welds demonstrate similar UTS (880 MPa) and YS (470 MPa) to that of the base metal, indicating a high-quality weld were achieved using the optimized parameters in this study. However, the elongation of the welds has reduced by about 12% compared to the base metal as shown in Figure 6b. This is correlated to the secondary phases such as Laves and MC in the FZ that degrades the mechanical properties and provides sites for crack initiation during loading. Both welds failed at the FZ and some micro porosities with the size of 50-150 μm were observed at the FZ. These pores could be another factor for reduced ductility of the welds compared to the base metal. Pore formation during laser

welding of IN718 is reported in other studies and its correlated to the poor fluidity of the Ni based alloys due to their high viscosity that results in entrapments of gas bubbles in the keyhole [11,12].

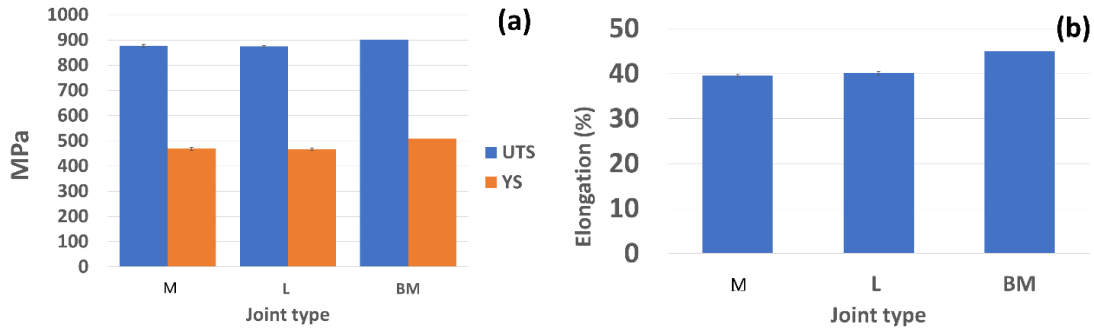


Figure 6. Mechanical properties of the weld and BM, UTS and TS (a) and elongation at break (b).

The fatigue strength of the welds at 10^6 cycles are shown in Figure 7. It can be seen that the M weld reveals superior fatigue strength than the L weld. This could be ascribed to the differences in fracture mechanism of the welds. The M weld fractured at the fusion line and deviated to the FZ (most of the fracture area is observed in the FZ), whereas, the L weld fractured at the HAZ and deviated toward the base metal. The microfissures and possible thermal impact of the laser cutting on the HAZ of the L weld could be the reason for its failure at the HAZ [13]. However, this needs further investigation to fully understand the microstructural changes in the HAZ of such a weld.

The fracture surface of the welds is depicted in Figure 8. It can be seen that the L weld fractured in a brittle manner due to the presence of the cleavages at the fracture surface (Figure 8 a and b), whereas the M weld reveals a ductile fracture due to the presence of the dimples at the fracture surface (Figure 8 c and d).

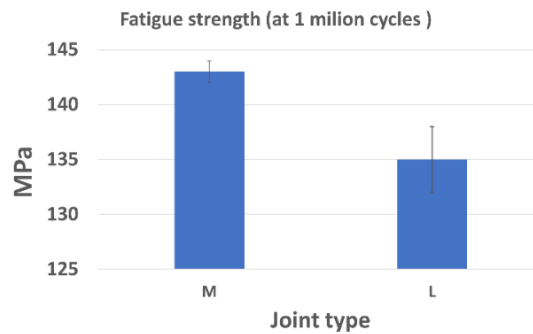
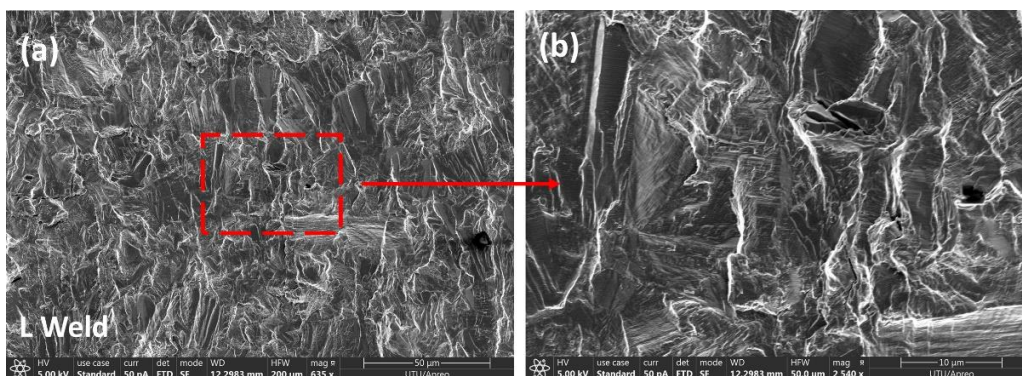


Figure 7. Fatigue strength of the welds.



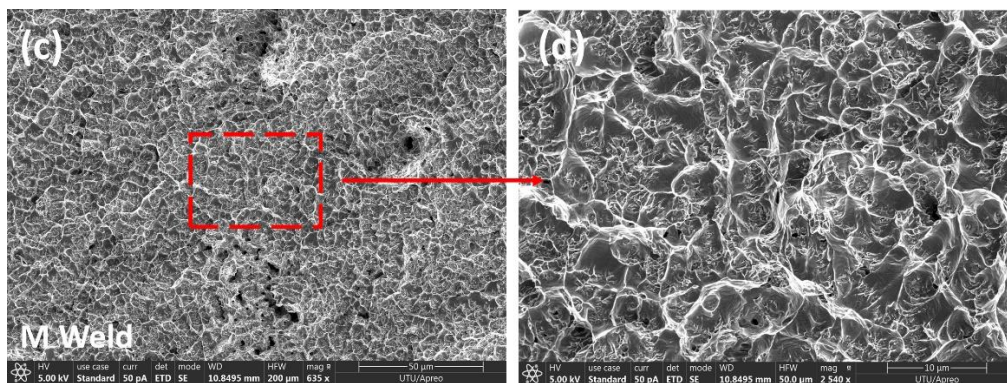


Figure 8. Fracture surface of the L weld (a,b) and M weld (c,d).

4. Conclusion

This study investigated the influence of laser and machined cut edge morphology on the mechanical properties of the wrought IN718 welds. It was indicated that the L weld possesses larger FZ than the M weld due to the higher cut edge roughness resulting from the laser cutting process, thus improving the absorptivity of the laser beam. Mechanical properties of the welds such as UTS and YS were comparable in both welds regardless of the difference in their joint edge morphology. However, the fatigue strength of the M weld revealed to be superior to that of the L weld. The results of this study demonstrate that the joint edge morphology could impact the fatigue strength of the welds, while other mechanical properties such as UTS and YS could be comparable regardless of their joint edge preparation.

Acknowledgments

The authors would like to thank Business Finland for funding this study via CaNeLis project as well as VADILA project funded by European Regional Development Fund. The authors would like to thank the University of Oulu for conducting the tensile and fatigue tests.

References

- [1] Shin J.S, Song K.H, Oh S.Y, Park S.K, 2024, Laser cutting studies on 10-60 mm thick stainless steels with a short focus head for nuclear decommissioning *Optics & Laser Technology* Volume 169, 110121.
- [2] Thomas D.J, 2016 Optimizing laser cut-edge durability for steel structures in high stress applications, *Journal of Constructional Steel Research*, Volume 121, Pages 40-49, ISSN 0143-974X.
- [3] Diekhoff P, Hensel J, Nitschke-Pagel T, Dilger K, 2020 Investigation on fatigue strength of cut edges produced by various cutting methods for high-strength steels. *Weld World* 64:545–561.
- [4] Chozaki S.P, Piili H, Afkhami S, *et al.* 2025 Investigation of the microstructure and mechanical properties of dissimilar joints of PBF-LB/IN718 to AISI 316L by laser welding. *Weld World*.
- [5] Maxwell DC, Nicholas T 1999 A rapid method for generation of a Haigh diagram for high cycle fatigue. In: *Fatigue and Fracture Mechanics: 29th Volume*. ASTM International.
- [6] Kaplan A.F.H. 2012 Local absorptivity modulation of a 1 μ m-laser beam through surface waviness, *Applied Surface Science*, Volume 258, Issue 24, Pages 9732-9736, ISSN 0169-4332.
- [7] Farokhi F, Nielsen S.E, Schmidt R.H, Pedersen S.S, Kristiansen M, 2015 Effect of Cut Quality on Hybrid Laser Arc Welding of Thick Section Steels, *Physics Procedia*, Volume 78, Pages 65-73.
- [8] Cao X, Rivaux B, Jahazi M, Cuddy J, Birur A 2009 Effect of pre- and post-weld heat treatment on metallurgical and tensile properties of Inconel 718 alloy butt joints welded using 4 kW Nd:YAG laser, *J. Mater. Sci.* 44. pp.4557–4571.
- [9] Sumit K, Sharma K, Biswas A.K, Nath I, Manna J, Majumdar D 2020 Microstructural change during laser welding of Inconel 718, *Optik*, Volume 218, 165029, ISSN 0030-4026.
- [10] Radhakrishna C.H, Prasad Rao K, 1997 the formation and control of Laves phase in superalloy 718 welds, *J. Mater. Sci.* 32 1977–1984.
- [11] Parchegani S, Piili P, Ganvir A, Salminen A, 2023 *IOP Conf. Ser: Mater. Sci. Eng.* 1296 012030.
- [12] Li, Y, Feng, Y. *et al.* Investigation on the Morphology and Formation Mechanism of Porosity in Different Heat Source Regions of Nickel-Based Alloy Laser Hybrid Welding. *J. of Materi Eng and Perform.*
- [13] Oreste S, D'Incau B, Zanon G, Raso S, Scardi P 2017 Laser and mechanical cutting effects on the cut-edge properties of steel S355N, *Journal of Constructional Steel Research*, Volume 133, Pages 181-191, ISSN 0143-974X.